Ion Channels in Biomembranes and Their Mimics

Ion Channels in Biomembranes and Their Mimics:

A Bioelectrochemical-Biophysical Approach

By

Rolando Guidelli

Cambridge Scholars Publishing

Ion Channels in Biomembranes and Their Mimics:
A Bioelectrochemical-Biophysical Approach

By Rolando Guidelli

This book first published 2022

Cambridge Scholars Publishing

Lady Stephenson Library, Newcastle upon Tyne, NE6 2PA, UK

British Library Cataloguing in Publication Data
A catalogue record for this book is available from the British Library

ISBN (10): 1-5275-8242-6
ISBN (13): 978-1-5275-8242-2

For my grandchildren
Neri and Petra

CONTENTS

Preface xi

1 Introduction 1

2 Structure and function of tetrameric ion channels 8
2.1 Patch clamping 10
2.2 Potassium channels 15
2.3 Sodium and calcium channels 20
2.3.1 Extracellular loops 21
2.3.2 Intracellular loops and the endogenous blocker 22
2.4 Inactivation after prolonged depolarization 23
2.5 The gating charge 24
2.5.1 The Boltzmann function 26
2.6 Sigmoidicity and the Cole-Moore effect 27

3 Modeling of tetrameric cation channels 29
3.1 Stochastic models 29
3.2 A deterministic model 31
3.2.1 The aggregation process 33
3.2.2 The inactivation phase and the ON ionic current 36
3.2.3 The ON gating charge 40
3.2.4 The OFF ionic and gating currents 43
3.2.5 Inactivation after prolonged depolarization 45

4 Sequence of conformational states in tetrameric ion channels 48
4.1 Sequence during the action potential 48
4.2 Sequence during depolarization and repolarization 53

5 The proton channels 57
5.1 Chord and slope conductance 60
5.2 Protomers and proton-conducting voltage sensing domains 61
5.3 Dimeric proton channels 65

6 Voltage-gated peptide channels 70
6.1 Bilayer lipid membranes (BLMs) 73
6.2 Modeling of voltage-gated peptide channels 82
6.2.1 The two-state model 83
6.2.2 The three-state model 84
6.3 Ionic current vs. potential curves 87
6.4 Ionic current vs. time curves 94

7 Techniques for biomimetic membranes 100
7.1 Scope and requirements 100
7.2 Optical techniques 104
7.2.1 Surface plasmon resonance 108
7.2.2 Polarization modulation infrared reflection absorption spectroscopy 111
7.2.3 Neutron reflectivity 115
7.3 Scanning probe microscopy techniques 120
7.3.1 Atomic force microscopy 120
7.3.2 Scanning tunneling microscopy 123
7.4 Other non-electrochemical techniques 129
7.4.1 Langmuir-Blodgett and Langmuir-Schaefer techniques 129
7.4.2 Quartz crystal microbalance 131
7.4.3 Vesicle preparation and fusion 134
7.4.3.1 Vesicle fusion on hydrophilic surfaces 136
7.4.3.2 Vesicle fusion on hydrophobic surfaces 137
7.4.3.3 Vesicle fusion on gold surfaces 139
7.5 Electrochemical techniques 141
7.5.1 Potential step chronocoulometry 141
7.5.2 Cyclic voltammetry 145
7.5.3 Potentials of zero free charge and zero total charge 150
7.5.4 The role of the DPTL thiolipid 152
7.5.5 Electrochemical impedance spectroscopy 155
7.5.5.1 Electrochemical impedance spectroscopy of Hg-supported tethered BLMs 161
7.5.5.2 Electrochemical impedance spectroscopy of solid-supported tethered BLMs 167
7.5.6 AC voltammetry 171
7.6 The absolute potential scale 173
7.6.1 Absolute potential difference across the Hg|water interface 174
7.6.1.1 A mercury-supported self-assembled lipid monolayer 174
7.6.1.2 Potential difference across a mercury-supported lipid SAM 177

7.6.1.3 The surface dipole potential of DOPC, DOPS, and DOPA 185
7.6.2 Absolute potential difference across Hg|water, Ag|water, and Au|water interfaces 188
7.6.2.1 Surface dipole potential χ_{TEO} of the DPTL tetraethylenoxy spacer 188
7.6.2.2 Absolute potential difference across lipid bilayers tethered to metal electrodes 192

8 Biomimetic membranes for ion channels 196
8.1 S-layer stabilized bilayer lipid membranes 196
8.2 Solid supported bilayer lipid membranes 199
8.2.1 The packing parameter 204
8.2.2 Different types of channel-forming peptides 207
8.2.3 Peptide ion channels in supported bilayer lipid membranes .. 211
8.3 Metal-supported tethered bilayer lipid membranes 219
8.3.1 Anchorlipids 223
8.3.2 Lateral mobility of lipids in tethered BLMs and floating BLMs 226
8.3.3 Gold- and mercury-supported DPTL|phospholipid tethered BLMs: a comparison 228
8.4 Solid-supported tethered bilayer lipid membranes 232
8.4.1 Compact tethered bilayer lipid membranes 232
8.4.1.1 Thiolipid based tethered bilayer lipid membranes 232
8.4.1.2 Tethered BLMs using anchorlipids different from thiolipids 248
8.4.2 Sparsely tethered bilayer lipid membranes 252
8.4.2.1 Thiolipid based sparsely tethered BLMs 252
8.4.2.2 Thiocholesteryl based sparsely tethered BLMs 264
8.4.3 1-thio-β-D-glucose based BLMs: floating BLMs 266
8.5 Mercury-supported tethered bilayer lipid membranes 274
8.5.1 Preparation of mercury-supported DPTL|lipid tethered BLMs 274
8.5.2 Modeling peptide channel formation at mercury-supported tethered BLMs 275
8.5.3 Modeling cyclic voltammetric behavior of mercury-supported tethered BLMs 279
8.5.4 Peptide ion channels at mercury-supported tethered BLMs 285

Abbreviations 322

References 324

Index 360

PREFACE

This book is largely based on my work on modeling of peptide and tetrameric ion channels carried out over the past five years with a significant contribution from Lucia Becucci, who started working with me on mercury-supported biomimetic membranes as a student in 1992 and has been conducting research in this area until recently, demonstrating notable skillfulness in organizing and carrying out research work and in devising stimulating experiments. The contribution from Giovanni Aloisi must also be mentioned. The book is accessible to graduate students and final year undergraduate students in chemistry and biology, as well as researchers in related disciplines including biology, physics, physiology, and pharmacology. It is also of interest to many electrochemists attracted by the biological realm and wishing to get a better view of the potentialities of their own background and tools to move more closely into this area. On the other hand, it is of interest to biophysicists and biochemists willing to get an exhaustive overview of the potential of solid-supported biomimetic membranes for the investigation of the function of channel-forming peptides and proteins using surface sensitive techniques. It is particularly suitable for students attracted by the fascinating area of biological membranes and their functions and interested in reading a text that takes practically no argument for granted and leads the reader, step by step, through gradually more fundamental aspects of this area.

The book deals with the bioelectrochemistry and biophysics of biological membranes and of their mimics in a homogeneous and thematically unified way. It is by no means a collection of selected, separate topics on the subject. After an Introduction section, which briefly summarizes the content of the whole book, this is composed of seven chapters. In Chapter 2, the biophysical techniques employed to investigate the tetrameric ion channels in biomembranes are described. The structure and function of the most widely investigated tetrameric ion channel, namely the Shaker K^+ channel, are then outlined and the many common features shared with Na^+ and T-type Ca^{2+} channels are emphasized, together with the unavoidable differences. Chapter 3 deals with the modeling of tetrameric ion channels. Stochastic models are only briefly touched upon, due to the high number of free parameters involved. Conversely, the deterministic two-state model of tetrameric K^+, Na^+ and T-type Ca^{2+} channels and the

three-state model of peptide ion channels, which require two, or at most three, free parameters are treated in a unified way by specifying all steps of the mathematical procedure. The resulting system of four or five differential equations can be easily solved by Runge-Kutta Fortran programs available in the literature using a desktop or laptop computer. The short Chapter 4 is devoted to the important and rather controversial issue of the sequence of conformational states assumed by ion channels during depolarization, repolarization, and action potential. Chapter 5 deals with dimeric proton channels and their protomers. Particular emphasis is placed on the role played by the time dependence of the open probability during chronocoulometric potential steps, which allows current vs. time curves of families of protomers to be simulated with a single free parameter. Chapter 6 is devoted to the quantitative interpretation of experimental current vs. potential and current vs. time curves of peptide ion channels by a three-state model, which constitutes a generalization of the two-state model of tetrameric ion channels. Here, too, a correct interpretation of chronocoulometric current vs. time curves requires the time dependence of the open probability to be adequately accounted for. Chapter 7 provides a qualitative description of several techniques commonly adopted for the investigation of peptide ion channels. Besides outlining optical, electrochemical, and scanning probe techniques, a brief review of Langmuir-Blodgett transfer, quartz crystal microbalance and vesicle fusion is provided. In addition, the absolute potential difference across Hg|water, Ag(111)|water, and Au(111)|water interfaces is estimated, by anchoring the same DPTL thiolipid to different noble metal surfaces. This achievement is required not so much to compare the behavior of an ion channel reconstituted in a biomimetic membrane with that already known from biomembranes or conventional BLMs, but to convey novel information about the behavior of ion channels within a biomembrane. Ultimately, Chapter 8 describes the fabrication of different biomimetic membranes and their use for the incorporation of peptide ion channels and for application of the techniques described in the preceding Chapter to many selected peptide ion channels. Particular emphasis is placed on lipid bilayers supported by hydrophilic solid surfaces and tethered bilayer lipid membranes supported by Au(111) and Hg electrodes. Advantages and disadvantages of Hg over Au supports are listed.

I am very grateful to those publishers who allowed me to reproduce figures appeared in their own publications, with particular regard to the American Chemical Society. The source of each of these figures is indicated in the corresponding legend. Special thanks go to the Commissioning Editor Ms. Helen Edwards for her helpful advice and excellent editorial suggestions and to Ms. Amanda Millar for her precious help and constant

assistance during the preparation of the final proofs of the book. Needless to say, the responsibility for any shortcomings that remain is entirely my own.

1 INTRODUCTION

Living cells are enveloped by a selectively permeable barrier, the plasma membrane, which protects and shields the set of their life-sustaining chemical transformations from changes in the environment. For its normal activity, the plasma membrane must prevent undesirable agents from entering the cell, while keeping needed molecules on its inside. It must also selectively allow the passage of molecules, ions, and signals from one side of the membrane to the other. Ion transport is mediated by protein-lined channels called *ion channels*. Ion transport through ion channels is an example of passive transport because permeant ions are moved from the membrane side where their electrochemical potential is higher to that where it is lower (Guidelli, 2017).

In view of the presence of aqueous media on both sides of biomembranes and bilayer lipid membranes (BLMs), the electrochemical potential difference of a permeant ion between the extracellular and the intracellular side of a membrane can be regarded as the sum of the osmotic contribution $k_B T\ln(a_o/a_i)$ and the electrostatic contribution $ze\phi$. Here, k_B, T, and e are the Boltzmann constant, the absolute temperature, and the elementary charge, respectively; a_o and a_i are the ion activities on the extracellular and intracellular side of the membrane, z is the *charge valence*, and ϕ is the transmembrane potential. According to usage, ϕ is the electric potential on the intracellular side of the membrane with respect to that on the extracellular side, which is set equal to zero by convention.

The osmotic contribution tends to move ions from the membrane side where their activity a (or, as a first approximation, their concentration c) is higher to that where it is lower. On the other hand, the electrostatic contribution tends to move ions towards the intracellular side if ϕ has an opposite sign with respect to the ion charge ze or in the opposite direction if ϕ and ze have the same sign. Thermodynamic equilibrium is attained when $k_B T\ln(a_o/a_i)$ becomes exactly equal to $ze\phi$, yielding the expression for the *Nernst equilibrium potential* $\phi_{eq} = (k_B T/ze)\ln(a_o/a_i)$. The above considerations hold strictly for ion channels that allow the flow of a sole permeant ion species.

Ion channels fulfilling the above requirement are the voltage-gated K^+, Na^+, Ca^{2+} and H^+ channels. The first three ion channels consist of four units

and are referred to as *tetrameric ion channels*. Conversely, H^+ channels are formed by two identical monomeric units (*homodimers*). Their features differ from those of voltage-gated Cl^- channels, which have a completely different and scarcely known structure and are selective for different anions. Their name is due to Cl^- ion being the predominant anionic species in the extracellular fluid.

For typical values of the intra- and extracellular concentrations of K^+, Na^+, Ca^{2+} and Cl^- ions in a biological membrane, the corresponding Nernst potentials assume the following values:

$$\phi_{\mathrm{K}} = \frac{k_{\mathrm{B}}T}{e}\ln\frac{2.5\ \mathrm{mM}}{200\ \mathrm{mM}} = -110\ \mathrm{mV}; \quad \phi_{\mathrm{Na}} = \frac{k_{\mathrm{B}}T}{e}\ln\frac{200\ \mathrm{mM}}{10\ \mathrm{mM}} = +75\ \mathrm{mV}$$
$$\phi_{\mathrm{Ca}} = \frac{k_{\mathrm{B}}T}{e}\ln\frac{1\ \mathrm{mM}}{10^{-4}\ \mathrm{mM}} = +235\ \mathrm{mV}; \quad \phi_{\mathrm{Cl}} = -\frac{k_{\mathrm{B}}T}{e}\ln\frac{200\ \mathrm{mM}}{55\ \mathrm{mM}} = -33\ \mathrm{mV} \tag{1}$$

In the above equations, the numerator contains the extracellular concentration and the denominator the intracellular one. In practice, K^+ ions tend to pass from the intra- to the extracellular side of the membrane, leaving behind a defect of positive charges and causing the transmembrane potential ϕ to become negative. Conversely, Na^+ and Ca^{2+} ions tend to pass from the extra- to the intracellular side of the membrane, creating an excess of positive charges on the intracellular side and causing ϕ to become positive. Note that these excess charges are not uniformly distributed over the respective liquid phases but are in direct contact with the intra- or extracellular membrane surface. In view of the very low Ca^{2+} concentrations both inside and outside the plasma membrane, their role is minor and often completely neglected, as in the case of the action potential (cf. Sec. 4.1).

Under physiological conditions, all tetrameric ion channels tend to move their permeant cation from the membrane side where its concentration is higher to that where it is lower, i.e., against its concentration gradient. The transmembrane potential regulates the ion flow by opening or closing the ion channel. The current i flowing along a single tetrameric ion channel at a transmembrane potential ϕ is proportional to the difference between ϕ and the corresponding Nernst equilibrium potential ϕ_{eq}. The $i/(\phi-\phi_{\mathrm{eq}})$ ratio is termed *single channel conductance* and is usually denoted by γ. The product of γ by the *probability* p of the single ion channel being open and by the number of ion channels per unit surface area of the membrane (i.e., its *number density* N) yields its *specific conductance*, $G = Np\gamma$, namely the conductance per unit surface area of the membrane due to all ion channels of the given type.

In the presence of different tetrameric ion channels, the transmembrane potential ϕ in its *resting state* can be regarded as a weighted average of the Nernst potentials, ϕ_+ and ϕ_-, of the permeant cations and anions of all ion channels present in the membrane, where the weights are expressed by the specific conductances, G_+ and G_-, of the corresponding ion channels (De Felice, 1997):

$$\phi = \left(\sum\nolimits_+ G_+\phi_+ + \sum\nolimits_- G_-\phi_-\right)\Big/\left(\sum\nolimits_+ G_+ + \sum\nolimits_- G_-\right). \tag{2}$$

The subscripts + and – are extended to all voltage-gated cation and anion channels. This amounts to assuming that, in the immediate vicinity of the mouth of each ion selective channel, this tends to establish the equilibrium situation with respect to the corresponding permeant ion to an extent proportional to its specific conductance.

A voltage-gated K^+ channel opens, allowing a flow of permeant ions, by stepping the transmembrane potential ϕ from a negative resting potential to a sufficiently positive ϕ value. This potential step is called *depolarizing pulse* and the resulting process is named *depolarization*. The reverse, backward potential step (*repolarizing pulse*) triggers a process called *repolarization*. Analogous considerations hold for the other tetrameric ion channels.

Let us now envisage a physiologically relevant situation in which the membrane contains three different types of tetrameric ion channels, selective toward Na^+, K^+ and Cl^- ions. It is well known that the K^+ ion concentration in the cytoplasm is much higher than that in the extracellular medium, while the opposite is true for the Na^+ ion concentration. If only the three inorganic ions Na^+, K^+ and Cl^- were present, the Cl^- concentration would be the same inside and outside of the cell and equal to the sum of the Na^+ and K^+ concentrations, to ensure the local electroneutrality of the intra- and extracellular solutions. Actually, the cytoplasm also contains bulky negatively charged molecules, such as adenosine triphosphate (ATP) and adenosine diphosphate (ADP), which cannot permeate the plasma membrane and cooperate with Cl^- ions to counterbalance the charge of potassium and sodium ions. This explains why the Cl^- concentration is higher in the extracellular medium. The resting transmembrane potential is the weighted average of the Nernst potentials of the three tetrameric ion channels:

$$\phi = \left(G_{\mathrm{K}}\phi_{\mathrm{K}} + G_{\mathrm{Na}}\phi_{\mathrm{Na}} + G_{\mathrm{Cl}}\phi_{\mathrm{Cl}}\right)\Big/\left(G_{\mathrm{K}} + G_{\mathrm{Na}} + G_{\mathrm{Cl}}\right). \tag{3}$$

During their function, tetrameric and proton ion channels undergo a series of conformational changes. The reason for the rather late appearance of 3D structures of these ion channels resides in the notable difficulty in crystallizing proteins that have both membrane-spanning and water-exposed parts. In some cases, a sufficient amount of high-quality purified protein has allowed the structure of some conformations to be determined from X-ray diffraction data and, more recently, by the use of cryogenic electron microscopy. Thus, Long et al. (2005) reported the X-ray crystal structure of a mammalian Shaker K^+ channel $K_v1.2$ at 2.4 Å resolution. A structure of a eukaryotic voltage-gated Na^+ channel Na_vPaS from American cockroach at 3.8 Å resolution was reported by Shen et al. (2017) using cryogenic electron microscopy. A cryogenic electron microscopy structure of human $Ca_v3.1$ called $Ca_v3.1$-Δ8b, with a deletion within the I-II loop and 3.3 Å resolution, was reported by Zhao et al. (2019). The structure of all the above tetrameric ion channels includes a *selectivity filter* (SF), which is in charge of allowing the passage of the sole permeant cation of the corresponding tetrameric ion channel. It controls the inflow and outflow of the permeant cation, while being located on the extracellular side of the central pore of the tetrameric ion channel.

Voltage-gated ion channels are also formed by several peptides. Most of them are *amphiphilic* α-helical peptides, namely peptides with one side of the helix lined with a number of amino acid residues having polar side chains. As a rule, these peptides tend to be initially adsorbed flat on top of membranes. Then, when the intracellular side of the membrane becomes sufficiently negative, they turn the positive pole of their α-helix (the *N-terminus*) normal to the surface of the membrane and penetrate it. There, they aggregate into clusters with the polar side of their α-helix turned towards the lumen of the cluster and the hydrophobic side turned towards the surrounding lipid molecules, giving rise to a peptide ion channel. A typical example is offered by the peptaibole alamethicin (Eisenberg et al., 1973).

Peptides can also form *ohmic ion channels*. These channels allow the passage of permeant ions across the membrane in both directions, depending on the sign of the transmembrane potential. When the transmembrane potential ϕ is negative, possible permeant cations move into the intracellular side of the membrane across the ion channel, while possible permeant anions move in the opposite direction. The situation is reversed if ϕ is positive. In both cases a plot of the current I against ϕ crosses the ϕ axis at $\phi = 0$ and is linear in the proximity of this point. If the solutions that bath the two sides of the membrane have identical composition, this plot remains linear throughout the whole accessible ϕ range. Several voltage-gated and ohmic peptide ion

channels show a certain selectivity for ions. However, differently from tetrameric ion channels, such a selectivity is not confined to a single ionic species but extends to a few ions of usually the same charge.

A peculiar example of ohmic channel is offered by gramicidin (Gr) (Rostovtseva et al., 1998). The helix of this unique channel-forming peptide differs from the α-helix of most channel-forming peptides and proteins in that its lumen is large enough to allow the passage of simple desolvated monovalent cations. Since its length is about one half that of a biomembrane, it spans it by forming a dimeric channel. Gr is selective for monovalent cations, with the following order of decreasing selectivity: $NH_4^+ > Cs^+ > Rb^+ > K^+ > Li^+$. It is also selective for Tl^+ ions, which are believed to bind specifically to Gr channels (Shvinka and Caffier, 1988). Gr moves these cations in one direction or the other, depending on the sign of the transmembrane potential. Observed deviations of current vs. potential curves from linear behavior when moving away from $\phi = 0$ are ascribed to the kinetics of dimerization (Bamberg and Läuger, 1973; Becucci et al., 2007). A rare example of ohmic channel formed by aggregation of monomeric peptide molecules is the lipodepsipeptide syringopeptin 25A (SP25A) (Dalla Serra et al., 1999).

Other ion channels are the *ligand-gated ion channels*. These ion channels open or close in response to the binding of a small signaling molecule termed *ligand*. Some of them are gated by extracellular ligands, and some others by intracellular ones. In both cases, the ligand is not the molecule that is transported when the channel opens. Ligand-gated ion channels are outside the scope of this book.

An enormous amount of electrophysiological and electrochemical methods has been devised to investigate the functional activity of ion channels and its relationship with their structure. The most direct method for studying tetrameric and proton ion channels consists in clamping a very tiny patch of a cell membrane and recording single channel currents across this patch. This method, called *patch clamping*, avoids the necessity of isolating and purifying the protein under study but requires the elimination of interfering proteins by suitable inhibitors. Introduction of purified DNA encoding wild-type tetrameric ion channels into eukaryotic cells (*transfection*), followed by patch clamping, is also employed (Finol-Urdaneta et al., 2014). On some occasions large proteins have also been incorporated into artificial membranes called *bilayer lipid membranes* (*BLMs*), which consist of a lipid bilayer spanning a very small hole in a hydrophobic septum interposed between two aqueous solutions (Zakharian, 2013). If such an incorporation allows the protein to retain its functional activity, the term *reconstitution* is

sometimes employed. At any rate, BLMs are much more widely employed for the investigation of peptide ion channels.

BLMs are the simplest and most realistic biomimetic membranes. Unfortunately, they are very fragile and overly sensitive toward vibrations, mechanical shocks, and transmembrane potentials greater then 100 - 150 mV. Hence, in the early 1980s robust metal-supported biomimetic membranes started to be devised. They all terminate in a lipid bilayer that is brought in contact with a bathing aqueous solution during use. By far the most widely employed supporting metal is gold. Gold-supported biomimetic membranes lend themselves to investigation of peptide ion channels by several surface sensitive techniques, which provide useful information on their structure and on the orientation of the peptide molecules incorporated into the lipid bilayer moiety. On the other hand, the permeant ion flow across gold-supported biomimetic membranes is too low to be detected by electrochemical techniques such as cyclic voltammetry or potential step chronocoulometry. Only an AC technique such as electrochemical impedance spectroscopy (EIS) can be successfully employed, even though data interpretation suffers from some measure of subjectivity.

Use of mercury as a support for biomimetic membranes imparts to the lipid molecules of the lipid bilayer the same lateral mobility as that in biomembranes. Ion flow across Hg-supported biomimetic membranes is large enough to be easily monitored with all electrochemical techniques, such as potential step chronocoulometry and cyclic voltammetry. Lack of significant surface defects allows EIS experimental data to be interpreted using simple equivalent circuits. On the other hand, surface sensitive techniques are inaccessible to mercury supports, with the exclusion of a couple of techniques applicable to platinum tips coated with a thin film of electrodeposited mercury.

The material of this book is organized as follows. Use of patch clamping for the electrophysiological investigation of tetrameric ion channels is described first. Next, the common structural and functional features of the three tetrameric ion channels are examined, followed by their modeling. Stochastic models are only briefly outlined, whereas the deterministic model developed by Guidelli and coworkers is described in detail and accompanied by examples of experimental plots and their fitting. The same approach is then adopted with dimeric proton channels. Subsequently, methods of preparation of bilayer lipid membranes commonly employed for the investigation of peptide ion channels are briefly reviewed. Next, the experimental features of voltage-gated peptide channels are described, followed by their modeling with a significant variant of the model used with tetrameric ion channels.

Scope and requirements of biomimetic membranes and a brief description of their different types are then outlined. Before examining them in detail, the techniques most adopted for their characterization are reviewed. After a brief introduction to electromagnetic waves, a qualitative description of surface plasmon resonance (SPR), polarization modulation infrared reflection absorption spectroscopy (PM-IRRAS) and neutron reflectivity (NR) is provided. Next, the essential features of atomic force microscopy (AFM), scanning tunneling microscopy (STM), Langmuir-Blodgett (LB) and Langmuir-Schaefer (LS) transfers, quartz crystal microbalance (QCM) and vesicle fusion are examined. A description of some electrochemical techniques follows, namely potential step chronocoulometry, cyclic voltammetry, and AC voltammetry, with particular emphasis on electrochemical impedance spectroscopy (EIS).

Before examining several metal-supported biomimetic membranes, where the absolute potential difference across their lipid bilayer moiety (i.e., the transmembrane potential ϕ_m) is unknown because thermodynamically inaccessible, the problem relating this quantity with the thermodynamically significant transmembrane potential at biomembranes and BLMs must be considered. To this end, an absolute potential scale ϕ' capable of relating the electric potential E measured vs. some reference electrode (say, the SCE) at Hg-, Au- and Ag-supported biomimetic membranes with the transmembrane potential of biomembranes and BLMs is proposed. In this connection, the fundamental role played by a widely used thiolipid called DPTL is pointed out. At the end, many selected solid-supported bilayer lipid membranes (sBLMs) and tethered bilayer lipid membranes (tBLMs) are described, followed by a description of Hg-supported tBLMs.

2 STRUCTURE AND FUNCTION OF TETRAMERIC ION CHANNELS

The tetrameric K^+, Na^+, and Ca^{2+} ion channels share the main structural features, probably because they are likely to have evolved from common ancestor proteins, dating back to simple peptide ion channels. All of them consist of four units of high internal homology. In Na^+ and Ca^{2+} channels the units are connected by conformationally flexible loops and are called *domains*. The units of K^+ channels are not bound together and are referred to as *subunits.* Each unit consists of six membrane-spanning α-helices (S1 to S6). A schematic picture of the polypeptide chain of the four domains of Na^+ or Ca^{2+} channels is shown in Fig. 1a. The four units are circularly arranged around a transmembrane pore, as pictorially represented in Fig. 1b.

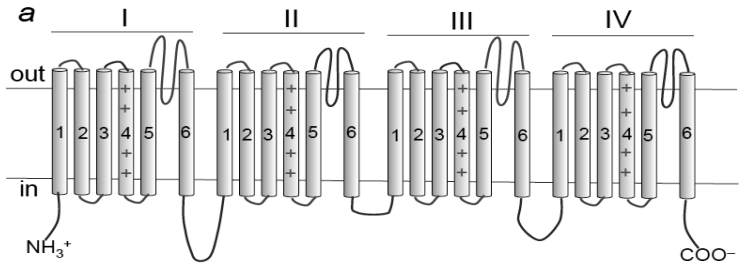

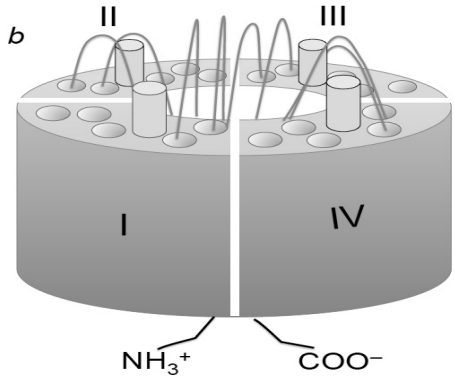

Figure 1. (*a*) Typical polypeptide chain of the four domains of a Na^+ or Ca^{2+} channel, each domain consisting of six transmembrane α-helices. Cylinders denote α-helices, curved lines connecting the cylinders denote intra- or extracellular loops. In K^+ channels, the loops connecting each domain to the subsequent one are missing. The fourth helix of each domain (S4) is positively charged and yellow-colored. (*b*) Schematic of the arrangement of the four domains (I-IV) of a tetrameric ion channel around the central pore; the S4 helices (yellow) are represented in the 'out' position, with the extracellular loop linking the S5 to the S6 α-helix of each domain folded back into the central pore.

Before entering the detail of tetrameric ion channels, it is expedient to examine the techniques employed to scrutinize their physiological behavior.

2.1 Patch clamping

The most common method to measure single-channel currents at a biomembrane is the *patch-clamp technique*, which owes its name to its use for clamping a patch of a cell membrane. This electrophysiological technique was developed in 1976 by Neher and Sakmann, who received the Noble Prize in Physiology or Medicine in 1991 for their work (Neher and Sakmann, 1976; Molleman, 2003). Since then, there has been a progressively increasing interest in exploiting its power to monitor ion channels in action in unprecedented detail. This technique can be applied to a wide variety of cells but is especially useful in the study of excitable cells, such as neurons and muscle fibers.

The glass micropipette employed with the patch-clamp technique has a tip inner diameter of about one micrometer and contains an aqueous solution and a AgCl-coated silver wire. The composition of this solution can be changed, and drugs can also be added to study ion channel behavior under different conditions. The micropipette is placed next to a cell, and a gentle suction is applied through it to draw a piece of the cell membrane (the *patch*) into the micropipette tip, as shown in Fig. 2. The patch seals the micropipette tip imparting to it a resistance of the order of gigaohms (1 GΩ = 10^9 Ω), which reduces the background electrical noise to one or few picoampères. The resulting configuration, with the intact cell clamped to the micropipette tip, is called *cell attached*.

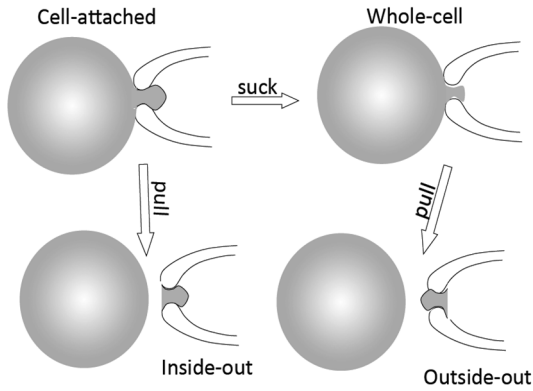

Figure 2. Different configurations of the patch-clamp technique, showing the micropipette tip and a cell. Firstly, a seal in the cell-attached configuration is formed. From this, whole-cell, perforated-patch, and inside-out configurations can be generated. The outside-out configuration requires starting from the whole-cell configuration. Source: Guidelli and Becucci, 2011a. Reprinted with permission from Springer.

The cell attached configuration is obtained at a high success rate and allows the investigation of the tiny patch of the membrane clamped by the pipette. Since the patch is *in situ*, it is expected to maintain structural integrity and intracellular modulation. However, the transmembrane potential is unknown, because both the Ag|AgCl quasi-reference electrode inside the pipette and the reference electrode in the bathing solution are located outside the clamped cell. If the transmembrane potential is regarded as stable, a reasonable guess of its value can be obtained from an investigation of the whole cell configuration (see below). The cell attached configuration can only be interrogated in the *single channel mode*, i.e., by recording single channel currents.

Starting from the cell-attached configuration, two alternative methods can be chosen to break the membrane patch spanning the pipette tip while maintaining the *gigaseal* intact. One method consists in applying a suction pulse by mouth through the pipette pressure tubing. This operation needs practice. The other method consists in delivering a large current pulse through the pipette. Some patch clamp amplifiers have a 'zap' function that carries out this operation. In this way, the Ag|AgCl electrode inside the pipette comes in direct contact with the cytosol. With this configuration, called *whole-cell* configuration, the content of the cell equilibrates rapidly with the solution inside the pipette, allowing a control of the ionic concentrations inside the cell. The area of the membrane under potential control is that enclosed between the Ag|AgCl electrode inside the micropipette and a reference electrode in the bathing solution. This area practically includes the whole cell membrane, with the obvious exclusion of the removed patch, and is clearly much greater than that of a patch. Consequently, the level of noise is too high to allow the recording of single channel currents, and only the overall current due to all the ion channels present in the cell membrane can be recorded.

Replacement of the cytoplasm by the pipette solution may not be appropriate, especially when the subject of study involves intracellular signaling, because whole-cell recording may dilute or even wash away crucial elements in the signaling cascade. This problem can be obviated starting from the cell-attached configuration and inserting *amphotericin B*, a channel-forming antibiotic peptide, in the solution inside the pipette. The antibiotic makes the patch permeable to small ions, but not to larger molecules such as the cAMP second messenger molecules. This configuration, called *perforated patch*, lowers the resistance of the patch to such an extent as to allow the recording of the current that flows across the whole cell membrane. As distinct from the whole-cell configuration, however, many constituents of the cytosol cannot diffuse into the solution

inside the pipette through the patch, thus preserving several properties of the cytosol.

Starting again from the cell-attached configuration with its *gigaseal*, the pipette can be gently pulled away, tearing the patch spanning the pipette tip. Nonetheless, the bond between the membrane and the pipette glass is stronger than the structural strength of the membrane. Hence, while the mild pull tears the patch, a tiny membrane fragment remains attached to the rim of the pipette tip, rapidly resealing its orifice. By so doing, the resulting patch exposes its intracellular, cytosolic side to the external solution, where it can be easily submitted to different experimental conditions. The resulting configuration is called the *inside-out patch*. In many instances, the bathing solution must be replaced with the intracellular solution to create an appropriate environment for the patch. This operation is time consuming and may cause the deterioration and death of the other cells in the bath. This *excised patch* configuration is clearly chosen if one aims to modulate the cytosolic side of the cell membrane.

In the opposite case in which it is the extracellular side of the cell membrane that one intends to modulate, the opposite excised patch is selected, called the *outside-out patch*. This is formed upon starting from the whole cell configuration, with the pipette filled with the intracellular solution. Next, the pipette is gently pulled away from the cell. The membrane will then break around the rim of the pipette tip and reseal to form a new patch, with the extracellular side turned toward the bathing solution. The latter solution does not need to be changed and the experiment can immediately start.

Electrophysiological measurements using cell-attached, inside-out and outside-out configurations involve only very tiny membrane patches, which contain one or only a few ion channels and require single channel recording. Conversely, whole-cell and perforated-patch configurations involve the whole membrane surface area and require whole-cell recording. The experimental set-up must account for the above differences. Single-channel recordings have a small signal-to-noise ratio and require a very effective noise control. The external noise must be undetectable, much lower than the intrinsic one. In addition, the intrinsic noise must be minimized, say, by reducing the stray capacitance.

Even under the most favorable experimental conditions, current noise is unavoidably determined by the thermal agitation of electrical charges and is inversely proportional to the resistance R of the film. Ohm's second law states that R is given by $R = \rho d/A$, where d is the film thickness, A is its surface area and ρ is a proportionality constant called *resistivity*. Since the membrane thickness d is not accurately known, the membrane resistance is

usually expressed by $RA = \rho d$, in $\Omega\ cm^2$. In practice, to record single channel currents, a membrane resistance of at least 2 GΩ is required. Since the resistance of a typical cell containing intrinsic proteins amounts to about 10^3 $\Omega\ cm^2$, the membrane area must be less than about 50 μm^2. Hence, the inner diameter of the pipette tip must be less than 8 μm. The sensitivity of recording is much less in whole-cell recording, where a 100- to 1000-fold decrease in sensitivity is required.

Recording of the opening and closing of single ion channels is obtained by applying the appropriate transmembrane potential between the Ag|AgCl reference electrode inside the pipette and an identical reference electrode in the bathing solution, using an inside-out or outside-out configuration. If, in addition to the protein under investigation, other proteins capable of interfering with the recording are present in the patch, specific inhibitors are used to block their function. The protein of interest is often expressed in the oocytes of the *Xenopus laevis* frog, which transcribe and translate the injected genetic information (Goldin, 2006). These oocytes are easily available, have large size and do not express many endogenous ion channels and receptors. Moreover, only some oocytes express endogenous channels, and it is frequently possible to obtain oocytes that do not show endogenous currents. In addition, the current induced from the injected RNA is usually much larger than that across the endogenous channels, so that it is generally possible to record the expressed exogenous current without significant contamination from native oocyte currents. Lastly, some channels can only be expressed in oocytes and not in mammalian cells.

Patch clamping is a laborious process that requires a skilled experimentalist to manipulate a glass micropipette under a microscope to record one cell at a time. Fertig et al. proposed a *planar patch clamping* technique for whole-cell recording, which does not require micromanipulation or visual control (Fertig et al., 2002). This technique makes use of glass-based planar patch-clamp chips of 200 μm thickness, with apertures of ~ 1 μm diameter. In conventional patch clamping, the micropipette tip is placed onto the surface of the membrane of a cell under optical control via a microscope. Then, a tight seal is established by gentle suction, and an omega-shaped protrusion of the membrane is drawn into the patch pipette (see Fig. 3a). In the case of a planar patch-clamp chip with a single aperture, a suspension of cells is placed on top of the chip. Next, application of a suction moves a single cell onto the aperture, as shown in Fig. 3b. As in conventional patch clamping, the membrane can then be ruptured for whole-cell access either with suction or voltage pulses. The result is an electrical connection to the inside of the cell allowing for current recording.

Microfluidic cartridges containing a glass substrate with several patch-clamp apertures, each of which individually addressable by microfluidic channels on both sides of the substrate, have been employed by Bao et al. (2008). This design allows perfusion of cells and compounds by robotic pipetting means, making the whole approach very suitable for automation. In the case of multiple apertures on a single chip, individual, feedback-controlled, suction lines are required for positioning and sealing of the cells. Besides scaling up the number of recording ion channels, the throughput capability is increased by automated application of drugs by a pipetting robot. A microarray design with several patch microfluidic channels on the sides of a large central microfluidic channel for cell delivery was also proposed by Seo et al. (2004), as schematically depicted in Fig. 3c. Cells injected in the patch channels are trapped by applying a negative pressure to these latter. This lateral design is claimed to allow efficient multiplexing of patch measurements, exchange of intracellular electrolytes while the cell is attached to the patch pore, and optical observation of membrane deformation.

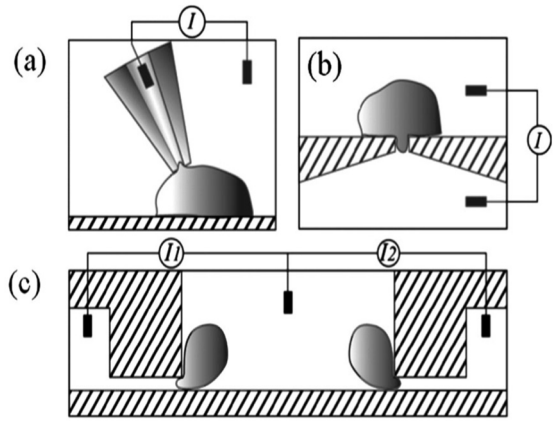

Figure 3. Different patch-clamp setups: (a) Traditional patch-clamp based on a glass micropipette. (b) Planar patch clamping. (c) Microarray design with patch microfluidic channels on the sides of a large central channel for cell delivery. A cross-section containing two patch sides is shown. The small black rectangles denote reference electrodes. Source: Seo et al., 2004. Reprinted with permission from the American Institute of Physics.

Other widely employed biomembrane models are the *liposomes* (also called *unilamellar lipid vesicles*). They are spherical lipid bilayers, a few tens of nanometer in diameter, which enclose an aqueous solution. Lipid vesicles may be obtained by treating a lipid suspension in water with ultrasounds, a procedure called *sonication* (see Sec. 7.4.3). Due to their small size, they cannot be normally investigated by electrochemical techniques. Rather, they can be studied by spectroscopic techniques using fluorescent or spin labeled molecular probes. Remarkable exceptions are represented by giant unilamellar vesicles (GUVs), which can be clamped to the tip of an ultramicropipette, allowing their transmembrane potential to be varied by the patch-clamp technique.

2.2 Potassium channels

K^+ channels are the most extensively investigated tetrameric ion channels. Their mechanism of action is similar to that of the other tetrameric ion channels. Differently from Na^+ and Ca^{2+} ion channels, the four units of K^+ channels are not bound together and are referred to as *subunits*. The four subunits, arranged around a central conducting pore, may be identical, forming a *homotetramer*. There are also potassium channels formed by related, but not identical, protein subunits, giving rise to *heterotetrameric* complexes. In view of the great variety of potassium channels, they are grouped into *subfamilies*. Heterotetramers are only formed from different subunits participating in the same subfamily and show hybrid properties, intermediate between those of the corresponding homotetramers. Conversely, subunits from different subfamilies cannot combine to form heterotetramers. Since K^+ channels have been more thoroughly investigated than Na^+ and Ca^{2+} channels, we will first describe structure and function of K^+ channels, and we will then point out the main differences shown by the other two. Eventually, similar behavioral features of all three types of channels will be reviewed.

As a consequence of a depolarizing pulse, all tetrameric ion channels show a rapid initial increase of conductance lasting a few milliseconds, called *activation phase*. This is followed by a much slower decay of conductance, referred to as *inactivation phase*. The *squid axon K^+ channel* involved in the *action potential* (cf. Sec. 4.1) was originally named *delayed rectifier* because, following a depolarizing pulse, it first increases the membrane conductance with a relatively long delay and then, most importantly, experiences an exceptionally long decay of conductance, with a decay time constant of about 600 ms. This very long inactivation phase is not detectable during an action potential, where the curve of the K^+ current

against time attains an apparently constant plateau, having no time to decrease.

Conversely, many other K^+ channels, called A-type channels, exhibit a rapid inactivation phase. The first A-type K^+ channels were cloned from the fruit fly *Drosophila*. They are called *Shaker*, *Shal*, and *Shab*, and are characterized by progressively longer times of the inactivation phase, in the order. The vertebrate homologues of these three channels constitute the K_v1, K_v2, and K_v3 subfamilies (Hille, 2001). Inactivation can be removed by expressing the ion channel without the amino acids 6 to 46 of the N-terminus, yielding the so-called Shaker IR, where IR stands for 'inactivation removed'. In what follows, we will describe in detail the mechanism of action of the Shaker K^+ channel.

Voltage-gated K^+ channels consist of four identical or homologous subunits, each composed of six α-helical transmembrane segments (S1-S6). The four repeated subunits (I-IV) are assembled around a central pore (Long et al., 2005). The S4 segment of each subunit has four arginine residues (R1-R4), each alternated with two neutral amino acid residues. A depolarizing pulse induces the opening of K^+ channels by determining the outward movement of the four positively charged S4 segments across the transmembrane electric field, together with that of about 13 of their elementary charges *e* (*the gating charges*) (Catterall, 2010).

The outward movement of each S4 helix is accompanied by its rotation along a spiral path in such a way that the arginine residues form, sequentially, a series of ion pairs with the negatively charged residues of the corresponding S1, S2, and S3 segments. According to this *sliding helix* model of gating, the S4 segments respond to a positive shift of the transmembrane potential by rotating by about 60° and moving toward the extracellular side of the membrane by 4.5 Å, to bring each positive charge into alignment with the next negative charge. The 'substituted cysteine accessibility method' supports the view that each S4 segment moves through a narrow hydrophobic waist, called the *gating pore* or *gasket*, interposed between two hydrophilic vestibules, with the transmembrane electric field focused along its length, estimated about 10 Å. In consideration of their role, the four S1-S4 segments are referred to as a *voltage sensing domain* (VSD).

While each subunit forms a VSD with its own S1-S4 segments, its S5 and S6 segments contribute to the formation of the central *pore domain* (PD), together with the S5 and S6 segments of the three other subunits composing the K^+ channel. The VSDs are located at the corners of a square, with the PD at its center. They seem to be floating as separate domains from the PD, with the space interposed between the hydrophobic surface of the